Proceedings of the International Gas Turbine Congress 2003 Tokyo
November 2-7, 2003

IGTC2003Tokyo-TS-051

# Flow in a High Speed Compressor Due to Axisymmetric Tip Clearance

Hyun Suk Joo[1] and Seung Jin Song[2]

[1, 2] School of Mechanical and Aerospace Engineering
Seoul National University
Seoul 151-742, KOREA
Phone: +82-2-880-1667, FAX: +82-2-883-0179, E-mail: sjsong@snu.ac.kr

**ABSTRACT**

This paper presents an analytical study of radial flow redistribution in a high speed compressor stage with axisymmetric tip clearance. The flow is assumed to be inviscid and compressible. The stage is modeled as an actuator disc and the analysis is carried out in the meridional plane. Upon going through the stage, the radially uniform upstream flow splits into the tip clearance flow and the passage stream. The tip clearance flow is modeled as a jet driven by blade loading, or the pressure difference between the pressure and suction sides. Thus, the trajectory of the leakage flow is calculated from kinematics. Then the mass fraction of each stream and the strength of the shear layer between the two are found as functions of compressor parameters. The model takes into consideration the detached shock that occurs in the rotor passage. This shock model is used to calculate the change in flow variables.

**NOMENCLATURE**

| | |
|---|---|
| $C$ | absolute flow velocity |
| $c$ | axial blade chord; component of absolute flow velocity |
| $C_l'$ | lift coefficient per unit span |
| $C_p$ | pressure coefficient |
| $H$ | total enthalpy; annulus height |
| $h$ | enthalpy |
| $i$ | axial direction |
| $k$ | radial direction |
| $M$ | Mach number |
| $p$ | pressure |
| $Q$ | strength of shear layer |
| $q$ | nondimensional vorticity strength |
| $s$ | blade pitch |
| $t$ | radial tip clearance |
| $U$ | compressor rotational speed at the mean radius |
| $W$ | relative flow velocity |
| $x$ | axial direction |
| $y$ | tangential direction |
| $z$ | radial direction |
| $ZW$ | Zweifel coefficient |
| $\alpha$ | absolute flow angle |
| $\beta$ | relative flow angle |
| $\beta_m$ | mean flow angle |
| $\chi$ | blade dirction angle |
| $\gamma$ | specific heat ratio |
| $\Delta$ | thickness of underturned layer |
| $\phi$ | flow coefficient |
| $\lambda$ | nondimesional mass fraction of underturned flow |
| $\theta$ | degree of underturning |
| $\rho$ | density |
| $\omega$ | angular velocity of rotor shaft rotation |
| $\omega_y$ | vorticity of meridional flow |
| $\psi$ | meridional stream function |

Subscripts

| | |
|---|---|
| $ps$ | pressure side |
| $r$ | relative component |
| $ss$ | suction side |
| $t$ | stagnation condition |
| $-\infty$ | far upstream |
| 0 | IGV inlet |
| 1 | rotor inlet |
| 2 | stator inlet |
| 3 | stator exit |
| $+\infty$ | far downstream |
| $\perp$ | meridional component |

Superscripts

| | |
|---|---|
| – | flow which has crossed compressor rotor blades |
| + | flow which was underturned due to the rotor tip gap |


Manuscript Received on March 31, 2003

**INTRODUCTION**

Tip clearance flow refers to the flow that leaks through the gap between blade tip and the endwall. Various authors have investigated the effects of such a flow on the performance of axial turbomachinery. As the tip clearance increases, the pressure rise across the compressor decreases along with its efficiency. Also, the stalling flow coefficient increases. These trends can be seen in both low speed and high speed machines (MacDougal, 1988; Freeman, 1985). Various methods have been proposed to analyze flows and losses associated with the tip clearance. Rains (1954) first proposed the "jet" model, and suggested that the flow is driven by the pressure difference between the pressure side and the suction side before rolling up into a vortex. Losses were assumed to arise from the dissipation of some of the kinetic energy of the flow. This model requires experimental data to determine the vortex trajectory, and it does not consider the effects of such flow on the rest of the passage flow. Lakshminarayana (1970) suggested the idea of "retained lift" in which a portion of the blade loading is retained in the clearance flow. One weakness of the model is its inability to predict the amount of lift retained, or the strength of the tip vortex. Chen et al. (1990) has proposed a similarity analysis based on vorticity dynamics and accurately predicted the trajectory of the tip

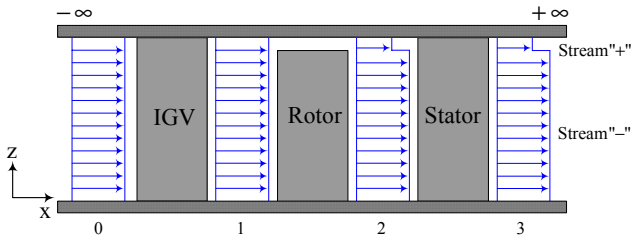

Fig. 1 Schematic view of a compressor stage

vortex. Song & Martinez-Sanchez (1997) proposed an alternative analytical model that solved for the flow associated with the tip clearance coupled with the rest of the passage flow in a turbine. The model focused on the interaction between the tip clearance flow and passage stream. Its predictions were found to compare well against Chen's prediction and experimental data. Increasingly, investigators are turning to CFD to better calculate tip clearance flows. Hah (1986), Adamczyk et al. (1989), and Crook (1989) fall into this category.

Much research on tip clearance flows in high speed machines has also been done. Suder et al. (1996) studied high-speed tip clearance flows both experimentally and computationally. Also Chima (1998) and Gerolymos et al. (1999) computed tip clearance flows in high speed machines and compared their CFD results with experimental measurements. However an analytical model for compressible flow response to tip clearance is still lacking. Therefore, the objective of this research is to develop a simple model to predict the radial redistribution of flow caused by rotor tip clearance in high speed compressors.

## MODEL DESCRIPSTIONS

The modeling approach is similar to that of Song & Martinez-Sanchez (1997). Analysis is axisymmetric and two-dimensional in the meridional plane. This model uses an actuator disk, and, thus the blade to blade details are ignored. Upon going through the actuator disc, the radially uniform upstream flow splits into two streams due to tip clearance. Stream "+" is associated with the rotor tip clearance, and stream "–" is called the main passage flow. The model assumes the flow to be inviscid and compressible without area change. The compressor geometry is assumed to be two dimensional at the mean radius values. The flow is assumed to follow the blades perfectly, and blockage and deviation are not accounted for in this model. It should be mentioned here that the focus of this analysis is not on loss but on the overall, inviscid flow kinematics.

The actuator disc in this study consists of an IGV row, a rotor blade row, and a stator blade row (Fig. 1). The IGV and the stator blade rows have full span blades while the rotor has partial span blades. Axial, tangential, and radial directions are denoted by $x$, $y$, and $z$, respectively. Upstream of IGV is referred to as Station 0. Inlet to the rotor is referred to as Station 1, and the rotor exit is called Station 2. Downstream of the stator row is called Station 3. Far downstream is referred to as $+\infty$. The compressor's rotational speed, absolute velocity, and relative velocity are $U$, $C$, $W$, respectively. $\alpha$ is the absolute flow angle, and $\beta$ is the relative flow angle.

### Tip clearance analysis

Martinez-Sanchez (1990) developed an incompressible inviscid turbine tip clearance flow model whose predictions agreed with the theory and data of Chen (1991). As proposed by Rains (1954), the tip clearance flow is modeled as a jet driven by the pressure difference between the pressure and suction sides. This jet then collides with an equal amount of passage flow before rolling up into a vortex. Consequently, this tip vortex forms a layer that is underturned relative to the passage flow. This turbine tip clearance model has been modified for compressors (Roh, 1997). Both turbine and compressor models assume incompressible flow;

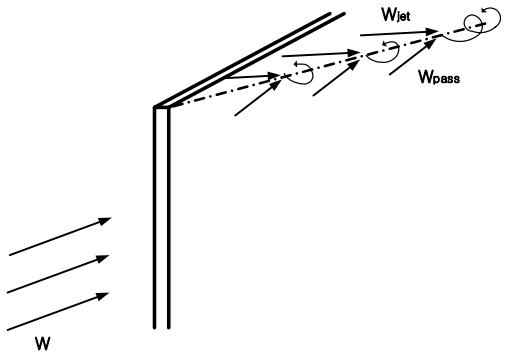

Fig. 2 The tip clearance flow model of Martinez Sanchez (1990)

therefore, they are valid only for low speed flows. However, Chima (1998) showed that the tip clearance flow in compressible flow regimes could be predicted by incompressible models. Therefore, Roh's tip clearance flow model is adopted in this study, and the model's details are given in the Appendix.

### Blade scale analysis

For compressible flows, the momentum equation can be written as

$$\nabla H_t + \vec{\omega} \times \vec{C} = 0 \tag{1}$$

where $H_t$ is the stagnation enthalpy defined as $H_t = h + C^2/2$, $\vec{\omega}$ the vorticity, and $\vec{C}$ the absolute velocity.

Also, due to the axisymmetric flow assumption $(\partial/\partial y = 0)$, the above equation reduces to

$$\vec{C}_\perp \cdot \nabla H_\perp = 0 \tag{2}$$

where $\vec{C}_\perp = \vec{i}\, c_x + \vec{k} c_z$ is the meridional velocity and $H_\perp = H_t - c_y^2/2$ is the meridional stagnation enthalpy.

The compressible form of continuity equation is

$$\nabla \cdot (\rho \vec{C}_\perp) = 0 \tag{3}$$

and continuity is satisfied by introducing a stream function $\psi(x,z)$ for the meridional flow as

$$c_x = \frac{\rho_1}{\rho}\frac{\partial \psi}{\partial z} \qquad c_z = -\frac{\rho_1}{\rho}\frac{\partial \psi}{\partial x} \tag{4}$$

At the rotor exit, the flow has split into two streams. For the passage stream (Stream "–"), the tangential velocities at the rotor and stator exit are, respectively

$$c_{y2}^- = U - c_{x2}^- \tan\beta_2 \tag{5}$$

$$c_{y3}^- = c_{x3}^- \tan\alpha_3 \tag{6}$$

Thus, the enthalpy rise for the passage stream is

$$\left(H_{\perp 3} - H_{\perp 1}\right)^- = h_3^- - h_1 - \frac{1}{2}c_{x1}^2\left[1 - \left(\frac{\rho_1}{\rho_3}\right)^2\right] \tag{7}$$

where $\rho_3$ is the density downstream of the stator.

For the underturned stream (Stream "+"), the tip clearance analysis predicts its azimuthal velocity to be

$$c_{y2}^{+} = U - c_{x2}^{+}\frac{\cos\theta\cdot\sin(\beta_m+\theta)}{\cos\beta_m} \tag{8}$$

where $\beta_m$ is the mean flow angle through the rotor and $\theta$ is the underturning of the Stream "+" relative to the Stream "–". Also at the stator exit,

$$c_{y3}^{+} = c_{x3}^{+}\tan\alpha_3 \tag{9}$$

Thus, the enthalpy rise for the underturned stream is

$$\left(H_{\perp 3} - H_{\perp 1}\right)^{+} = h_3^{+} - h_1 - \frac{1}{2}\left[c_{x3}^{+\,2} - \left(c_{x2}^{+}\frac{\sin\theta}{\cos\beta_m}\right)^2 - c_{x1}^2\right] \tag{10}$$

The fourth term on the right-hand side of above equation is included to account for the kinetic energy dissipated during the tip vortex formation. Then, the downstream vorticity between the underturned and passage stream can be determined as

$$\omega_{y3} = \frac{\rho_3}{\rho_1}\frac{\partial H_{\perp 3}}{\partial\psi} \tag{11}$$

To focus on the tip clearance effects, the coordinate system is transformed to the streamline coordinate from the z coordinate. Then, the equation for $\psi$ becomes

$$\begin{aligned} &\text{Upstream } (x<0)\ \nabla_{\perp}^2\psi = 0 \\ &\text{Downstream } (x>0)\ \nabla_{\perp}^2\psi = Q\delta(\psi-\psi_{tip}) \end{aligned} \tag{12}$$

Where $Q = \int_i^j \omega_y d\psi = H_{\perp 3}^{i} - H_{\perp 3}^{j}$ is the strength of azimuthal vorticity $\omega_y$ between stream *i* and *j*, and $\delta$ is Dirac's delta function.

The boundary conditions are

$$\begin{aligned} &\psi(x,0) = 0 && \psi(x,H) = \rho_0 c_{x0} H \\ &\psi(x=0-,z) = \rho_0 c_{x0} z && \frac{\partial\psi}{\partial x}(x=0+,z) = 0 \\ &\psi_1(z) = \psi_3(z) && \frac{\partial\psi_1(z)}{\partial z} = \frac{\partial\psi_3(z)}{\partial z} \end{aligned} \tag{13}$$

The strength of vorticities $Q$ in the shear layer is

$$\begin{aligned} \frac{\rho_1}{\rho_3}Q = {} & U\left(c_{y2}^{+} - c_{y1}\right) - U\left(c_{y2}^{-} - c_{y1}\right) \\ & - \frac{1}{2}\left(c_{y3}^{+\,2} + \left(c_{x2}^{+}\frac{\sin\theta}{\cos\beta_m}\right)^2 - c_{y3}^{-\,2}\right) \end{aligned} \tag{14}$$

Subsequently, the velocities at various axial locations can be determined. At the rotor exit, the axial velocities are

$$\frac{c_{x2}^{+}}{c_{x1}} = \frac{\rho_1}{\rho_2}\left(1 + \frac{1-\lambda}{2}\frac{\rho_3}{\rho_1}q\right) \tag{15}$$

$$\frac{c_{x2}^{-}}{c_{x1}} = \frac{\rho_1}{\rho_2}\left(1 - \frac{\lambda}{2}\frac{\rho_3}{\rho_1}q\right) \tag{16}$$

where $q = Q/c_{x1}^2$ and $\lambda$ is the nondimensional mass fraction of the underturned stream.

At the stator exit, the axial velocities are

$$\frac{c_{x3}^{+}}{c_{x1}} = \frac{\rho_1}{\rho_3}\left(1 + \frac{1-\lambda}{2}\frac{\rho_3}{\rho_1}q\right) \tag{17}$$

$$\frac{c_{x3}^{-}}{c_{x1}} = \frac{\rho_1}{\rho_3}\left(1 - \frac{\lambda}{2}\frac{\rho_3}{\rho_1}q\right) \tag{18}$$

One feature of the actuator disk approximation is that only half of the total change visible far downstream of the disk occurs at the disk while the other half occurs downstream. Therefore, far downstream of the stator, the axial velocities are

$$\frac{c_{x+\infty}^{+}}{c_{x1}} = \frac{\rho_1}{\rho_3}\left(1 + (1-\lambda)\frac{\rho_3}{\rho_1}q\right) \tag{19}$$

$$\frac{c_{x+\infty}^{-}}{c_{x1}} = \frac{\rho_1}{\rho_3}\left(1 - \lambda\frac{\rho_3}{\rho_1}q\right) \tag{20}$$

Substituting for velocities in the equation of the strength of vorticities yields a quadratic equation for Q as a function of blade geometry, the mass fraction of the underturned stream, and the density ratios as shown below.

$$\begin{aligned} &\left[(1-\lambda)^2 G + (1-2\lambda)\tan^2\alpha_3\right]\left(\frac{q}{2}\right)^2 + \\ &2\left[\frac{1}{\phi}\left(\frac{\rho_1}{\rho_2}\right)\left(\frac{\rho_3}{\rho_1}\right)\left(\lambda\tan\beta_2 + (1-\lambda)T\right) + \right. \\ &\left.\left((1-\lambda)G + \tan^2\alpha_3\right) + 2\left(\frac{\rho_1}{\rho_3}\right)\right]\left(\frac{q}{2}\right) + \\ &\left[\left(\frac{\rho_1}{\rho_3}\right)^2 G + \frac{2}{\phi}\left(\frac{\rho_1}{\rho_2}\right)\left(T - \tan\beta_2\right)\right] = 0 \end{aligned} \tag{21}$$

where $T = \frac{\cos\theta\cdot\sin(\beta_m+\theta)}{\cos\beta_m}$ and $G = \left(\frac{\sin\theta}{\cos\beta_m}\right)^2$.

Next, the underturned stream mass fraction can be determined from the given tip clearance as

$$\lambda = \frac{4\left(\frac{t}{H}\right)}{\left(1 - \frac{q}{2}\frac{\rho_1}{\rho_3}\right) + \sqrt{\left(1 - \frac{q}{2}\frac{\rho_1}{\rho_3}\right)^2 + 4\frac{q}{2}\frac{\rho_1}{\rho_3}\frac{t}{H}}} \tag{22}$$

Therefore, $\lambda$ and $q$ can be obtained if the density ratio in each stage is known.

In most high speed compressors, detached shocks occur in the rotor passage at the design point (Cumpsty, 1989), and, thus, rotor passage flow is unchoked. Freeman and Cumpsty (1992) developed a detached shock model by considering control volume extending from the inlet region to the maximum blade thickness location and solved the relation between the maximum blade thickness and the exit Mach number. However, in our model the entire blade passage is considered as the control volume (Fig. 3).

In the direction of blade chord, the continuity and momentum equations are conserved. Also, the relative total enthalpy is constant. Thus, from above relations, the rotor exit relative Mach number, $M_{r2}$, is easily obtained.

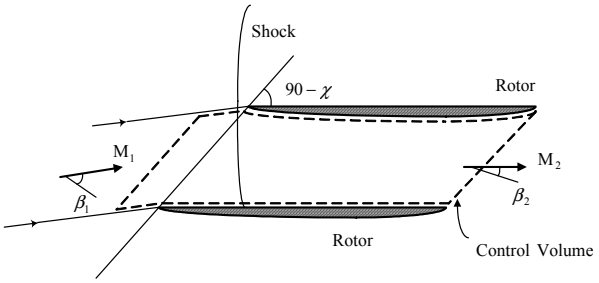


Fig. 3 Extended control volume considering entire rotor passage

$$\frac{\cos\chi+\gamma M_{r1}^2\cos\beta_1}{M_{r1}\cos\beta_1}\left(1+\frac{\gamma-1}{2}M_{r1}^2\right)^{-\frac{1}{2}} = \frac{\cos\chi+\gamma M_{r2}^2\cos\beta_2}{M_{r2}\cos\beta_2}\left(1+\frac{\gamma-1}{2}M_{r2}^2\right)^{-\frac{1}{2}} \tag{23}$$

where $\chi$ is a single blade direction. Therefore, the density ratio across the rotor is easily obtained.

$$\frac{\rho_2}{\rho_1}=\frac{M_{r1}}{M_{r2}}\left(\frac{1+\frac{\gamma-1}{2}M_{r2}^2}{1+\frac{\gamma-1}{2}M_{r1}^2}\right)^{\frac{1}{2}}\frac{\cos\beta_1}{\cos\beta_2} \tag{24}$$

In the stator, there is no shock in the flow, and the total enthalpy does not change. Thus, the density ratio across the stator is obtained from

$$\left(\frac{\rho_3}{\rho_2}\right)^{\gamma-1}+\frac{\gamma-1}{2}M_2^2\left(\frac{\rho_3}{\rho_2}\right)^{-2}\frac{\cos^2\alpha_2}{\cos^2\alpha_3} = 1+\frac{\gamma-1}{2}M_2^2 \tag{25}$$

where $M_2$ is the absolute mach number at rotor exit. From above results, the density ratio across the entire stage, $\rho_3/\rho_1$, is

$$\frac{\rho_3}{\rho_1}=\left(\frac{\rho_3}{\rho_2}\right)\left(\frac{\rho_2}{\rho_1}\right) \tag{26}$$

Therefore, from the prescribed tip clearance, $t/H$, the upstream stagnation conditions, and the obtained density ratios, above 2 equations can be solved for $q$ and $\lambda$.

Table. 1 Lewis single-stage compressor specifications at the design point

| Parameter | Value |
|---|---|
| $t/H$ | 0.02 |
| $s/c$ | 1.471 |
| $\alpha_1$ | 0° |
| $\beta_1$ | 56.53° |
| $\alpha_2$ | 45.31° |
| $\beta_2$ | 38.87° |
| $\alpha_3$ | 2.54° |

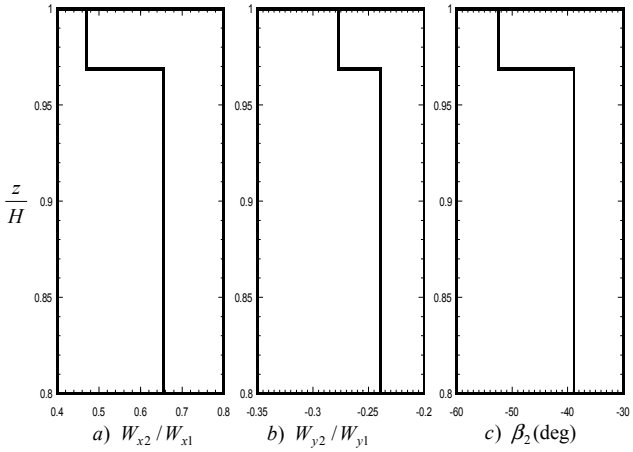


Figure 4 Radial distribution of (a) relative axial velocity; (b) relative tangential velocity; (c) relative flow angle

**MODEL PREDICTIONS**

The test compressor is a Lewis single-stage compressor described in Reid and Moore (1978, 1980). This compressor, called Stage 37, consists of rotor and stator. Table 3.1 shows the specifications of this compressor. Input upstream stagnation conditions are $P_{t1}$=101.4 kPa and $T_{t1}$=288.2 K. Also, the value of upstream Mach number and flow coefficient is 0.661 and 0.453, respectively. The tip clearance value is assumed to be 2 % of the annulus height.

Figs. 4a and 4b show the radial profiles of relative axial and tangential velocities at the rotor exit. $z/H$= 1 is the casing and $z/H$= 0 is the hub. The radially uniform upstream flow has split into two streams – the clearance stream and the passage stream. Due to the density increase across the rotor without area variation, the axial velocities at station 2 are smaller than those upstream of the rotor. Furthermore, relative to the passage stream, the clearance stream has a lower axial velocity (Fig. 4a) and a higher tangential velocity in the direction opposite to rotation (Fig. 4b). Thus, the clearance flow is underturned, and this can be seen in Fig. 4c that shows the radial profile of the relative flow angle at the rotor exit. The angle is defined to be positive in the direction of rotation. These effects are due to the kinematics of the tip clearance flow similar to the incompressible case.

Figure 5 shows the rotor exit flow field predictions from the new compressible model (solid line) and Roh's incompressible model (dashed line). Axial retardation and underturning of the

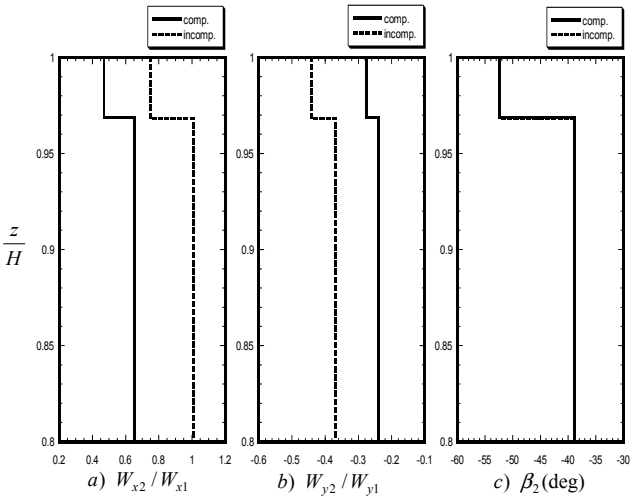


Figure 5 Radial distribution of (a) relative axial velocity; (b) relative tangential velocity; (c) relative flow angle predicted by compressible and incompressible models

clearance flow relative to the passage flow are similar in both cases. Since the tip clearance model is used in both models, the flow angle (Fig. 5c) and the mass fraction of the underturned stream remain the same. However, the downstream velocity magnitudes are smaller for the compressible downstream case due to the density increase (Figs. 5a and 5b).

Next, the prediction's sensitivity to tip clearance is analyzed. Fig. 6 shows a plot of the leakage flow vs. tip clearance for various Mach numbers. As the tip clearance increases, leakage mass flow increases proportionally. Velocity magnitudes and flow angles are not significantly affected; only the thickness of the underturned layer changes. Also, as seen in Fig. 6, the Mach number does not have much influence on the leakage mass fraction.

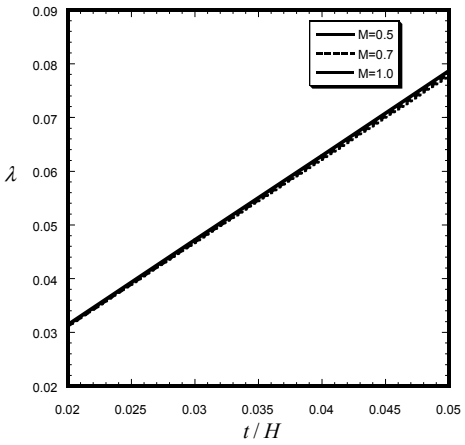


Figure 6 Leakage mass flow amount vs. tip clearance for the test compressor

## CONCLUSIONS

The intent of this study is to gain physical understanding of rotor tip clearance effects in high speed compressors, and an actuator disc model has been developed to illuminate such effects. The following conclusion can be drawn.

1) In compressible flows, as in incompressible flows, the underturned tip clearance flow has axial and tangential momentum defects relative to the passage flow.
2) The tip clearance variation mainly affects the mass fraction of the tip clearance, which increases linearly with tip clearance.

## REFERENCES


MacDougal, N. M., 1998, "Stall Inception in Axial Flow Compressors," Ph. D. Dissertation, University of Cambridge.

Freeman, C., 1985, "Effect of Tip Clearance Flow on Compressor Stability and Engine Performance," von Karman Institute for Fluid Dynamics, Lecture Series 1985-05.

Rain, D. A., 1954, "Tip Clearance Flows in Axial Flow Compressors and Pumps," CalTech Hydrodynamics Lab. Report No. 5.

Lakshminarayama, B., 1970, "Methods of Predicting the Tip Clearance Effects in Axial Flow Turbomachinery," ASME Journal of Basic Engineering, Vol. 104, pp. 467-481.

Chen, G. T., 1991, "Vortical Structures in Turbomachinery Tip Clearance Flows," Ph. D. Thesis, Department of Aeronautics and Astronautics, MIT.

Song, S. J., and Martinez-Sanchez, M., 1997, "Rotordynamic Forces Due to Turbine Tip Leakage: Part I – Blade Scale Effects," ASME Journal of Turbomachinery, Vol. 119, No. 4, pp. 695-703.

Hah, C. A., 1986, "Numerical Modeling of Endwall and Tip Clearance Flow of an Isolated Compressor Rotor," ASME Journal of Gas Turbine and Power, Vol. 108, No. 1, pp. 15-22.

Adamczyk et al., 1989, "Simulation of Three-Dimensional Viscous Flow Within a Multi-Stage Turbine", ASME Paper 89-GT-152.

Crook, A. J., 1989, "Numerical Investigation of Endwall/Casing Treatment Flow Phenomena," M.S. Thesis, Department of Aeronautics and Astronautics, M.I.T.

Suder, K. L., and Celestina, M. L., 1996, "Experimental and Computational Investigation of the Tip Clearance Flow in a Transonic Axial Compressor Rotor," ASME Journal of Turbomachinery, Vol. 118, No. 2, pp. 218-229.

Chima, R. V., 1998, "Calculation of Tip Clearance Effects in a Transonic Compressor Rotor," ASME Journal of Turbomachinery, Vol. 120, pp. 131-140.

Gerolymos, G. A., and Vallet, I., 1999, "Tip-Clearance and Secondary Flows in a Transonic Compressor Rotor," ASME Journal of Turbomachinery, Vol. 121, No. 4, pp. 751-762.

Martinez-Sanchez, M., and Gauthier, R. P., 1990, "Blade Scale Effects of Tip Leakage," GTL Report 202, MIT.

Roh, H. Y., 1997, "Blade Scale Effects of Tip Leakage Flow in Axial Compressors," B.S. Thesis, Department of Aerospace Engineering, Inha University.

Cumpsty, N. A., 1989, "Compressor Aerodynamics," Longman Scientific & Technical.

Freeman, C., and Cumpsty, N. A., 1992, "Method of the Prediction of Supersonic Compressor Blade Performance," Journal of Propulsion and Power, Vol. 8, No. 1, 199-208.

Reid, L., and Moore, R. D., 1978, "Design and Overall Performance of Four Highly Loaded, High-Speed Inlet Stages for an Advanced High-Pressure-Ratio Core Compressor," NASA TP-1337.

Moore, R. D., and Reid, L., 1980, "Performance of Single-Stage Axial Flow Transonic Compressor with Rotor and Stator Aspect Ratios of 1.19 and 1.26, Respectively, and With Design Pressure Ratio of 2.05," NASA TP-1659.


## APPENDIX

This appendix describes Roh's (1997) compressor tip clearance model. Fig. A1 shows this model schematically.

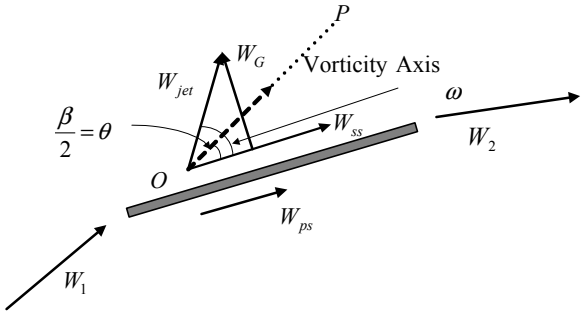


Fig. A1 Geometry of compressor tip vortex roll up (Roh, 1997)

The flow velocities on suction and pressure sides are obtained from the Bernoulli equation as

$$W_{ps} = \sqrt{W_1^2 - 2\frac{P_{ps} - P_1}{\rho}} \tag{A1}$$

$$W_{ss} = \sqrt{W_1^2 - 2\frac{P_{ss} - P_1}{\rho}} \tag{A2}$$

Also, for the flow through the tip gap,

$$W_G = \sqrt{2\frac{P_{ps} - P_{ss}}{\rho}} \tag{A3}$$

This gap flow then collide with an equal amount of passage

flow (Fig. 2). Since the flow is assumed to be inviscid, the two streams that collide have same total pressure, temperature, and also equal static pressures along their contact line. Therefore, these two streams must have equal velocity magnitudes, and the line OP bisects the angle made by $\vec{W}_{ps}$ and $\vec{W}_{jet}$.

Then,

$$\tan 2\theta = \frac{W_G}{W_{ps}} = \sqrt{\frac{C_{p_{ps}} - C_{p_{ss}}}{1 - C_{p_{ps}}}} \tag{A4}$$

where $C_p = \frac{P - P_1}{\rho W_1^2 / 2}$. Notice $C_l^{'} = C_{p_{ps}} - C_{p_{ss}}$, that and it can be shown that the degree of underturning of the vortex relative to the passage flow can be obtained as

$$\theta = \cos^{-1}\sqrt{\frac{4}{4 + C_l^{'}}} \tag{A5}$$

where

$$C_l^{'} = ZW\left(\frac{\cos\beta_2}{\cos\beta_1}\right) \tag{A6}$$

and *ZW* refers to the Zweifel coefficient

$$ZW = 2\left(\frac{s/c}{H/c}\right)\cos^2\beta_2\left(\tan\beta_1 - \tan\beta_2\right) \tag{A7}$$